

# A MASS SPECTROMETER

<b>INTRODUCTION</b>	<b>1</b>
<b>THEORY</b>	<b>1</b>
<b>THE MASS SPECTROMETER APPARATUS</b>	<b>3</b>
<i>Ion production and detection</i>	5
<i>Beam geometry, magnetic focusing, and mass resolution</i>	6
<i>Hall probe</i>	9
<i>Vacuum system requirements</i>	10
<b>PROCEDURE AND ANALYSIS</b>	<b>11</b>
<i>Data analysis</i>	13
<b>PRELAB PROBLEMS</b>	<b>14</b>
<b>APPENDIX A: THE BEAM FOCUSING MAGNET</b>	<b>A-1</b>
<i>Magnetic focusing</i>	A-1
<i>Magnetic field modeling</i>	A-2



## A MASS SPECTROMETER

### INTRODUCTION

The Lorentz force law for the electromagnetic field acting on a moving charge was derived from 19th century observations of the dynamics of macroscopic charged bodies and wires carrying currents (resulting from the net motions of enormous numbers of electrons). That this major result of classical electrodynamics theory is applicable to the dynamics of individual ions is a quite profound idea — that a theory founded on macroscopic, laboratory-sized objects is equally accurate for particles 23 orders of magnitude smaller. Using this theory one may construct an instrument which can create and then magnetically focus a stream of individual atomic ions. Such an instrument may be used to selectively detect ions of any particular mass, thus, for example, separating the various isotopes of a particular element and accurately determining their masses and relative abundances. This instrument is the *mass spectrometer*.

In this experiment you will use a simple mass spectrometer to observe the various isotopes of several alkali metals and halogens, testing the applicability of the Lorentz force law to individual ions of both positive and negative charge, and you will determine a value for  $e/m_{AMU}$ , the ratio of the electron charge to the *atomic mass unit* (AMU). Given a determination of  $e/m$  for the electron using the Zeeman effect (Experiment 27), you may then determine the ratio of the AMU to the electron mass.

### THEORY

Assume that the Lorentz force law, equation (9.1), and Newton's laws of motion are sufficient to describe the dynamics of an individual ion of charge  $q$  and mass  $m$  subject to the electric and magnetic fields present in the mass spectrometer. If the ions are well-separated and travelling through a good vacuum, then they will not be affected to any significant degree by the presence of other ions or gas molecules as they travel through the apparatus.

$$\vec{F} = \frac{d\vec{p}}{dt} = q\vec{E} + q(\vec{v} \times \vec{B}) \quad (9.1)$$

An inspection of (9.1) should convince you that a static magnetic field  $\vec{B}$  cannot do work on an ion, because the resultant force is perpendicular to the ion's motion. Thus  $\vec{B}$  cannot change the ion's kinetic energy. Ions are thermally generated in the instrument from salts deposited on a hot filament; they start with a charge of  $|q| = e$  and with kinetic energies of  $\sim 0.1$  eV (electron volt) and are subsequently accelerated by an electric field in the *ion gun*. The ions are accelerated

through a potential difference of  $V \approx 550$  volts, so they all have a kinetic energy of  $\approx 550$  eV, and speeds (depending on a particular ion's mass  $m$ ) given by (9.2).

$$v = \sqrt{\frac{2eV}{m}} \quad (9.2)$$

A charged particle moving with velocity  $\vec{v}$  in a uniform, static magnetic field  $\vec{B} \perp \vec{v}$  follows a circular path in a plane normal to  $\vec{B}$ . The radius  $R$  of the path of the particle's uniform circular motion is given by:

$$qvB = F = ma = m \frac{v^2}{R} \rightarrow BR = \frac{v}{q/m} \quad (9.3)$$

This circular path is now called *cyclotron motion* (after the *Cyclotron*, an early [1932] particle accelerator developed at UC Berkeley).  $R$  may be called the *cyclotron radius* of the motion. The angular frequency,  $\omega_c = v/R = (q/m)B$ , of the circular motion is called the *cyclotron frequency* and is obviously independent of the particle's speed (for nonrelativistic motion only!). More generally a charged particle will follow a helical path with its axis parallel to  $\vec{B}$ . This motion is responsible, for example, for the capture of solar wind particles and cosmic ray protons by the Earth's magnetic field (these captured particles cause the *Van Allen radiation belts*, discovered in 1958); their interactions with the atmosphere and the stronger magnetic fields near the poles cause the *auroras*.

For an ion with charge  $e$  and speed given by (9.2), we have:

$$\boxed{BR = \sqrt{\frac{2V}{e/m}}} \quad (9.4)$$

For this experiment we control the values of  $B$  and  $V$ , and  $R$  is fixed by the geometry of the magnet generating  $B$ . Using (9.4) we can determine  $e/m$  values for the various isotopes in the sample salts deposited on the ion gun filament.

## THE MASS SPECTROMETER APPARATUS

The mass spectrometer apparatus and its control electronics are shown in Figure 1 and Figure 2.

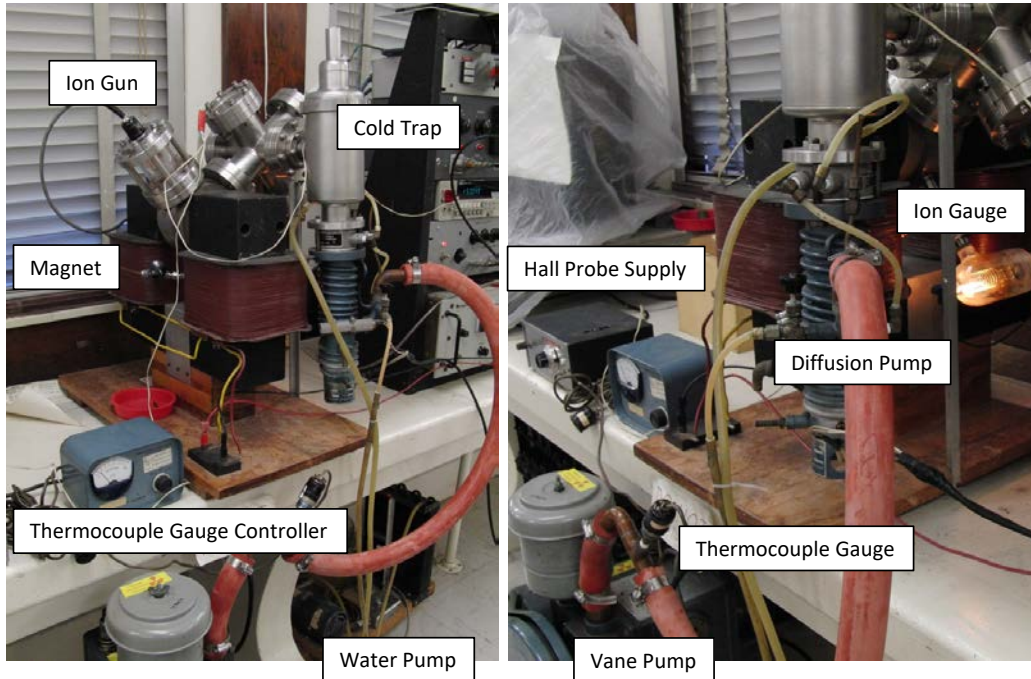


Figure 1: Two views of the typical mass spectrometer apparatus set-up with notable parts labeled. The actual set-up may use a different vacuum pump and pressure sensors from those shown.

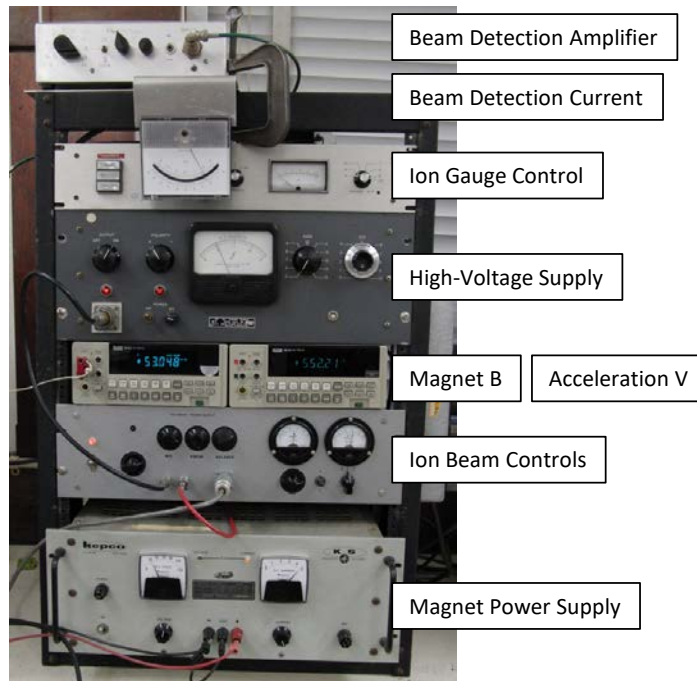


Figure 2: An example of the mass spectrometer control electronics. The actual electronics devices may be different, but their required functions will be the same.

The ion gun, ion detector, and focusing magnet comprise the heart of the instrument. These elements are shown in Figure 3, and a schematic view of the ion path through the instrument is provided by Figure 4.

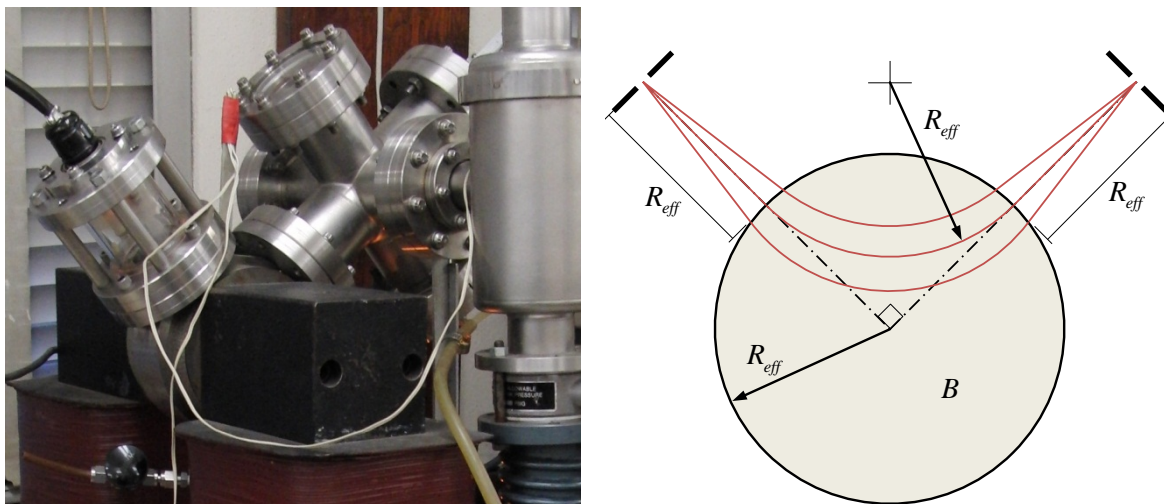


Figure 3 (left): Close-up of the ion gun, magnet poles, and ion detector. The photo also shows where the Hall probe is inserted to measure the magnetic field at the center of the gap between the pole pieces.

Figure 4 (right): A diagram of the path the ions take from the ion gun (upper left) to the ion detector (upper right). The beam is turned through  $90^\circ$  and focused by the magnetic field  $B$ , which is perpendicular to the plane of the figure. With the geometry shown, focusing is accomplished only for those ions whose cyclotron radius is equal to the effective radius of the magnetic field,  $R_{eff}$ .

The mass spectrometer is prepared for use by placing a small water droplet containing a mixture of a variety of salts on a filament in the ion gun, and the filament is heated to evaporate the water from the sample. The ion gun is reassembled and attached to the apparatus, and the mass spectrometer is then pumped down to a pressure of  $< 10^{-4}$  Torr before use.

Ions are emitted by the salts when the filament is heated in the vacuum of the instrument. The ions are accelerated toward a narrow exit slit in the ion gun by a potential difference established between the filament and the slit. They then coast through a region free of electric fields and enter the space between the focusing magnet poles. If the magnetic field in this region and the accelerating voltage in the ion gun are set correctly, the theory, equation (9.4), predicts that ions with a particular mass will turn through  $90^\circ$  and then exit the magnetic field. They then coast to the detector, a narrow entrance slit followed by a collecting plate. The ions are neutralized at this plate, and the current between this plate in the detector and the hot filament in the gun is measured. This current (in electron charges/second) is equal to the ion flux entering the detector slit.



of charge transfer for a particular element in the sample should vary according to a Boltzmann factor (see General Appendix B for a brief discussion of this topic):

$$\text{rate of ion creation} \propto e^{-E_{ion}/k_B T} \quad (9.5)$$

Heating the filament to  $\sim 1500$  K will result in  $k_B T \sim 0.13$  eV, whereas the ionization potential  $E_{ion} \sim 4$  eV  $\sim 30 k_B T$ . Consequently, the rate of ion creation is much larger for atoms whose  $E_{ion}$  are relatively small. In addition, small changes in filament temperature can result in very large changes in ion flux. The filament is heated by passing a current of  $\sim 1.5$ – $2.5$  Amps through it. The current must be very well-regulated by the filament power supply, or there could be large, random fluctuations in the ion flux. You control the filament current (and thus the filament temperature) using the ion beam control unit (Figure 2).

Ions in the beam which are focused by the magnet (as in Figure 4) enter another slit which defines the entrance to the ion detector. Behind this slit is a collector plate, as mentioned previously. When a positive ion strikes this plate it will stick to it and eventually pick up an electron from the metal and be neutralized; a negative ion will eventually give up its charge to the metal. A sensitive current amplifier connects the plate to ground potential, and its output is used to measure this charge transfer as ions enter the detector through its slit. The beam current meter and the current amplifier are shown in Figure 2; the ion beam current is typically a few times  $10^{-13}$  amps when the instrument is properly set up and an isotope is detected.

### ***Beam geometry, magnetic focusing, and mass resolution***

The mass spectrometer uses a  $90^\circ$  beam-focusing electromagnet as shown in Figure 3 and the simplified diagram in Figure 4. In our instrument the magnet pole-pieces are cylindrical with a radius of 2.5 inches and are separated by 0.4 inches, and the beam slits are  $\approx 2.5 \times 10^{-3}$  inches wide. A Hall probe is inserted into the pole-piece gap very near the field axis so that the magnetic field may be accurately measured.

The ion beam exits the ion gun slit with an angular spread of  $\sim 15^\circ$ , so some sort of beam focusing is required to provide a detectable signal. Using the magnet to turn the beam as shown in Figure 4 provides this focusing if the ion gun and the detector are oriented correctly and are at the proper distances from the axis of the pole pieces. Magnet focusing is discussed in this experiment's Appendix A; in this section we discuss how to use the  $90^\circ$  geometry with equation (9.4) to determine the  $e/m$  value for an ion you detect.

First assume the simple situation depicted in Figure 4: the magnetic field  $\vec{B}$  is uniform within a cylinder of radius  $R_{eff}$  and vanishes elsewhere, with the field direction parallel to the cylinder axis. An ion travels toward the cylindrical field along a line passing through the field axis and in a plane perpendicular to it. As the ion enters the field it begins to follow a circular path with a



cyclotron radius  $R$  given by (9.4). If the ion's path is such that it exits the field after turning by  $90^\circ$  and again along a line through the field axis, then it must be the case that  $R = R_{eff}$ . Thus, according to the theory, the field's effective radius  $R_{eff}$ , along with its magnitude  $B$  and the ion gun acceleration voltage  $V$  determine the  $e/m$  value for those ions who may successfully be detected. Adjusting  $B$  and  $V$  would allow you to scan through a range of  $e/m$  values, looking for ion detections.

The actual situation is more complex, because, of course, the magnetic field cannot be uniform within a cylinder between the pole pieces and suddenly drop to zero at the cylinder's edge. Since there are no sources of the magnetic field in the space between the pole pieces, the field may be described by a scalar potential  $\Phi_M$  which satisfies Laplace's equation,  $\nabla^2\Phi_M = 0$ , in this space. Even so, the actual field, as you might expect, is quite uniform over most of the volume between the poles as long as they are closely spaced, and the permeability of the pole piece metal is large. A numerical solution for the field in the plane through the middle of the gap as a function of distance from the axis is shown in Figure 6. Of course, by symmetry the field direction at all points in this plane must be perpendicular to it (i.e., parallel to the cylinder axis), although at other points between the poles away from the axis the field will have a radial component.

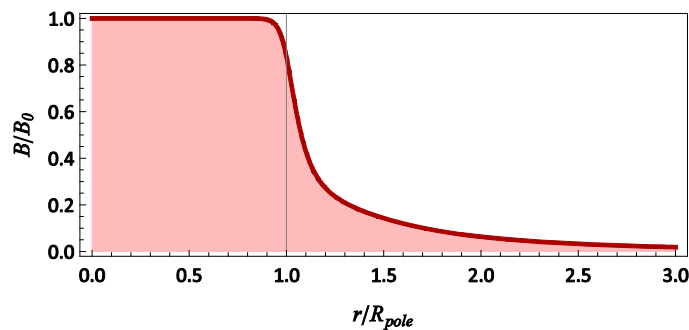


Figure 6: Results of a numerical model of the magnetic field in the plane midway between the pole pieces. The field is quite uniform for  $r < 0.9R_{pole}$ , but then decreases to about 5/6 of its center value at the pole piece radius. At large radii the field approaches that of a magnetic dipole, falling as  $r^{-3}$ . Clearly the field is not insignificant for  $r > R_{pole}$ , and thus the effective field radius  $R_{eff} > R_{pole}$ .

This experiment's Appendix A also describes how the magnetic field was modeled using a finite-difference relaxation method to numerically solve Laplace's equation for the pole gap geometry; *Mathematica*® notebooks with the actual model code are available on the sophomore lab website: [http://sophphx.caltech.edu/Physics\\_6/Extras/Mass\\_Spectrometer\\_Exp\\_9/Field\\_Models.zip](http://sophphx.caltech.edu/Physics_6/Extras/Mass_Spectrometer_Exp_9/Field_Models.zip).

As is clear from Figure 6, the magnetic field's magnitude remains appreciable at radii greater than the physical pole-piece radius, so the ions will start to be deflected from their initial path before entering the pole-piece gap. Consequently, a smaller magnetic field between the pole pieces will be required to complete the  $90^\circ$  turn of the ions as shown in Figure 7 (page 9–8). The Hall probe measures  $B_0$ , the field magnitude on the pole-piece axis (note from Figure 7 that the detected ions don't actually come very close to this axis). For a magnetic field varying with distance from the

pole axis as shown in Figure 6, the required ion cyclotron radius in the field between the pole pieces for the remainder of the  $90^\circ$  turn would be increased to  $1.158 \times R_{pole}$ , reducing the required field from that shown in (9.4) for the case of  $R = R_{pole}$ , the pole-piece physical radius.

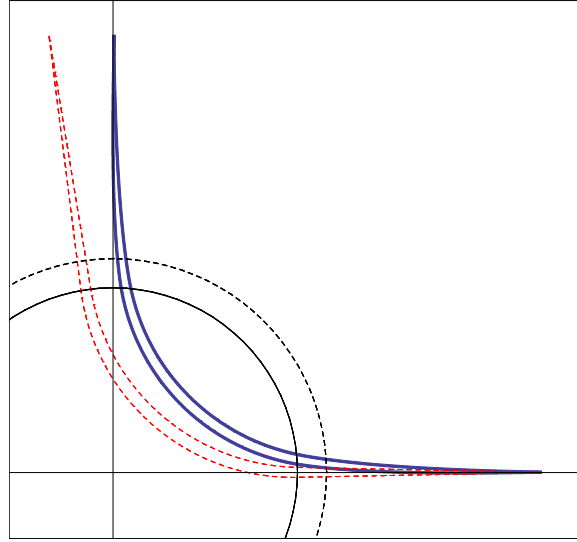


Figure 7: Because the magnet's field extends beyond its pole piece edges, a weaker central field is sufficient to turn the beam through  $90^\circ$ . The solid blue trajectories show ions under the influence of a numerically modeled field with value  $B_0$  at the pole center. On the other hand, the dashed red trajectories would be followed if the field were completely uniform and equal to  $B_0$  within  $R_{pole}$  and 0 elsewhere. In this latter case, to turn the beam through  $90^\circ$  and match the blue trajectories the pole-piece radii would have to be increased to  $R_{eff} = 1.158 \times R_{pole}$ , as shown by the dashed black circle. Note the focusing of the beam trajectories by the magnet.

We can, however, continue to use equation (9.4) assuming that  $B = B_0$ , the field at the pole axis, if we set a nonzero, constant  $B_0$ -field radius of  $R = R_{eff}$ , called the magnet's *effective field radius*: in this case a numerical model estimates  $R_{eff}$  to be:  $R_{eff} = 1.158 \times R_{pole}$ . For the spectrometer's physical pole radius of 2.5 inches, we then get:

$$\boxed{R_{eff} = 1.158 \times 2.50 \text{ in} = 7.35 \text{ cm}} \quad (9.6)$$

This is the value of  $R$  to use in equation (9.4) when analyzing the experiment data.

Finally, we estimate the mass resolution of the spectrometer. Consider the lateral displacement at the position of the ion detector of the exit beam away from the desired  $90^\circ$  exit path if we were to change the mass of an ion by a small amount. Rather than using the more accurate numerical field model, it turns out that we can get fairly accurate results by using our original, simplified field geometry model (Figure 4) with  $R_{eff}$  given by (9.6). Assume that  $B$  and  $V$  have been set so that ions of mass  $m$  enter the detector. Ions of a slightly different mass  $m + \Delta m$  would have a slightly different cyclotron radius. We calculate this change in radius (to first order) by differentiating equation (9.4):

$$\frac{1}{R} \frac{\partial R}{\partial m} = \frac{1}{2m} \rightarrow \frac{\Delta R}{R_{eff}} \approx \frac{1}{2} \frac{\Delta m}{m} \quad (9.7)$$

For relatively small changes in ion mass, the cyclotron radius is still very close to  $R_{eff}$ , and the angle through which the ions are turned by the magnet is very close to  $90^\circ$ . In fact (calculating everything to first order in  $\Delta m/m$ ), where the beam exits the magnetic field it will be displaced laterally by a distance of  $\Delta R$  and will have a velocity angle of  $\Delta\theta = \Delta R / R_{eff}$  away from  $90^\circ$  ( $\pi/2$ ). Thus after coasting to the detector a distance of  $R_{eff}$  further, the ions will be laterally displaced by a total distance of  $2 \times \Delta R$  from the position of the exit slit, which is an angular displacement of  $\Delta\theta$  (measured from the magnet pole center). Each slit (ion gun and detector) subtends an angle of  $w / 2R_{eff}$  ( $w$  is the slit width), and the sum of these two slit widths determines the best possible angular resolution of the instrument.

In order to prevent ions of mass  $m + \Delta m$  from entering the detector, we must have  $\Delta\theta > w / R_{eff}$ ,  $\therefore \Delta R > w$ . So the mass resolution of the instrument (to first order, assuming everything is perfectly aligned and focused) could be as good as

$$\frac{\Delta m}{m} > \frac{2w}{R_{eff}} \quad (9.8)$$

### ***Hall probe***

A Hall probe is used to accurately measure the magnetic field in the gap on the pole-piece axis. The probe you will use has some red tape on one end — in Figure 3 (page 9–4) you can see that end of it showing while it has been inserted into a slot on top of the magnet.

The Hall probe sensor is a small, thin, rectangular semiconductor wafer. Current  $I_H$  from a power supply flows across the wafer from one edge to the opposite, and the voltage  $V_H$  across the other two edges is measured by a sensitive voltmeter. Ideally, the measured  $V_H$  is proportional to the product of the component of the magnetic field normal to the surface of the wafer,  $B_\perp$ , and the current  $I_H$ , because the Lorentz force (9.1) causes the charge carriers in the wafer to be deflected by  $B_\perp$  toward one edge as they travel through it. This build-up of mobile charge carrier density along one edge in the (overall neutral) piece of material creates an electric field orthogonal to the direction of current flow, which is sensed by  $V_H$ .

You calibrate the hall probe in two steps:

- (1) Hold the probe far from any magnets and with its plane oriented parallel to the Earth's field. In this case  $V_H = 0$ . Use the offset or null function of the voltmeter attached to the probe to zero out any residual voltage reading.

- (2) Insert the probe into the calibration magnet (a small, permanent magnet) and adjust the Hall probe power supply current until the measured  $V_H$  corresponds to the value of the calibration magnet field  $B$ .

Keep the calibration magnet away from the spectrometer's electromagnet so that you don't change its magnetization!

### *Vacuum system requirements*

The ions cannot travel from the ion gun to the detector if they are very likely to hit some obstacle in their path. Air molecules (mostly  $N_2$  and  $O_2$ ) at normal atmospheric densities can be very effective at disrupting a beam of ions, so we must remove most of the air molecules from the ion path. We accomplish this by putting the system under vacuum, pumping away a large fraction of the air. Let us now estimate how much of the air we must remove.

Assume that we have an ion beam of cross-sectional area  $A$  passing through a very thin section of obstacles with density  $n$  (per unit volume). Assume that if an ion's center of mass comes within a distance  $b$  to an obstacle particle's center of mass, then it will be scattered (knocked off-course) by a large angle, effectively removing it from the ion beam. If it doesn't come within distance  $b$  of an obstacle, then its path is not affected (this scenario is an instance of *hard-sphere scattering*). Thus each obstacle particle presents a target of cross-sectional area  $\sigma = \pi b^2$  to the ions.  $\sigma$  is called the *total scattering cross-section* for our particular ion-obstacle situation.

If the section's thickness is  $dz$  along the ion path, then the average number of obstacle particles the beam would encounter is  $n \times A dz$ . This number times the scattering cross section gives the total area blocked by the obstacle particles in the section, and the fraction of ions which are scattered by the thin section is the ratio of this area to  $A$ , the cross-sectional area of the beam. The fraction of ions scattered is thus  $n \sigma dz$ , and the fraction  $1 - n \sigma dz$  make it through the section. Since we have a very thin section so that  $n \sigma dz \ll 1$  and we know that  $e^{-x} \rightarrow (1 - x)$  for  $x \ll 1$ , we conclude that the probability that an ion will not be scattered when traversing a finite distance  $z$  filled with target particles of density  $n$  and scattering cross-section  $\sigma$  is

$$\text{Probability of *not* being scattered} = e^{-n\sigma z} \quad (9.9)$$

This turns out to be the correct formula, which you may derive by integrating the differential relation. The length  $1/n\sigma$  is called the *mean free path*. A tolerable level of scattering must be assigned in order to determine the maximum allowable density of air particles,  $n$ , along the ion path. Using the ideal gas law  $P = n k_B T$ , we can then determine the maximum allowable pressure to which the vacuum system must pump down our instrument.

## PROCEDURE AND ANALYSIS

With the spectrometer electromagnet current set to 0, calibrate the Hall probe and then insert it into the slot on the top of the spectrometer electromagnet. Check the system pressure: if the pressure is too high, consult with your TA and the laboratory instructor. If using the apparatus ion gauge, its reading is only accurate while the spectrometer electromagnet is set to 0 current (why do you think that might be?).

**Heating the ion gun filament causes ions to be emitted.** All of the sample's various elements are being emitted by the filament, not just the particular one you are attempting to detect! A hot filament will emit those elements with a low ionization potential at a prodigious rate. Keep the filament current small when you are not actively using the spectrometer, and look for low ionization potential elements first, or they may be depleted from the sample before you look for them.

Check that the polarities of the magnet, high-voltage power supply, and beam detection amplifier are correctly set for *positive ion detection* (the alkali metals). Refer again to Figure 2 on page 9–3 to identify the various spectrometer controls.

*With the filament heating current set to 0*, adjust the electromagnet field by increasing the current on the magnet power supply (use the supply's constant current mode). Activate the high-voltage power supply and set the acceleration voltage to 550 V using the fine adjust knob. Use the voltmeters measuring the Hall probe voltage and the ion gun acceleration voltage to precisely set up the spectrometer. The beam detection amplifier should initially be set to its  $3 \times 10^{-13}$  Amp scale and its reading nulled using its *zero set* knob.

With  $B$  and  $V$  properly set for your first candidate element, gently heat the filament by setting the filament current to 1.6–1.8 Amps. After a few seconds, you should detect the ion beam. If not, slowly adjust the acceleration voltage away from 550 V until you find it. Adjust the filament heater current to keep the beam detector reading from exceeding the  $3 \times 10^{-13}$  Amp scale. Note how slowly the detector output responds to changes you make. Record the  $B$  and  $V$  values at the ion detection current peak.

A very weak detection implies that possibly:

- (1) The magnet current polarity and/or the high-voltage polarity are incorrect, or the magnet current is not set to the proper value (off by a factor of 10, maybe?).
- (2) The filament sample has been depleted of the isotope you are looking for.

- (3) You are looking for an element which is hard to ionize rather than one of the easily ionized ones.
- (4) The ion gun focusing needs to be adjusted. Consult your TA or the laboratory instructor for advice on how to do this procedure.

Estimate the voltage width of the ion peak by adjusting the acceleration voltage to determine its full width at half-maximum. Slightly change  $B$  and then adjust  $V$  to reacquire the ion peak. Record a few  $(B, V)$  combinations for this isotope.

Proceed up the alkali metal periodic table column looking for *the most abundant isotope* of each of the other elements. Reset  $B$  to the value you calculated in your prelab problem set. Once you find an isotope of an element, look for the other isotope(s) by leaving  $B$  set and adjusting  $V$  only (as you calculated in the prelab problems). You may need to use a higher filament current to detect the hard-to-ionize elements. Make sure you get a few data points for each isotope.

By changing the instrument quickly between two isotopes of the same element using the  $V$  control, you can use the detector currents at the peaks to estimate the relative abundance of the isotopes in the sample. Why is this? Why would this result be misleading, however, as a comparison of the relative abundance of two different elements in the sample?

After recording sufficient data for as many alkali metal isotopes as you can find, and near the end of the laboratory session period, you may now attempt to detect isotopes of chlorine and bromine. Because these are halogens, they can only be emitted as negative ions. With the magnet current set to 0 and the acceleration voltage deactivated (don't turn either of these power supplies off!), you may reverse the polarities of the magnet, acceleration voltage, and detection amplifier (make sure you understand why all three polarities require reversal). Look for the more abundant chlorine isotope first. You will probably need a filament heater current of a little over 2 Amps. Be patient! See if you can find this isotope before the lab instructor has to find it for you.

Determine the voltage width of the halogen peak for comparison with your alkali metal width.

Securing the instrument at the end of lab: reduce the magnet and filament currents to zero and deactivate the high-voltage power supply. Return polarities to the proper values to detect positive ions. Put the Hall probe sensor in the calibration magnet and recheck its calibration. **Do not turn off any of the electronics!** Deactivate the ion vacuum gauge (if necessary). **Leave the vacuum pumps on.**

### *Data analysis*

You will use your data to:

- (1) Check the validity of the Lorentz force law for the dynamics of the ions you have studied.
- (2) Determine a value (with uncertainty) for  $e/m_{AMU}$ , the ratio of the electron charge to the atomic mass unit (AMU).

Assume that each isotope's atomic mass  $m = W \times m_{AMU}$ , where  $W$  is the isotope's *Atomic Weight*, an integer (such as in  $^{133}\text{Cs}$  or  $^{87}\text{Rb}$ ). The actual atomic masses for your isotopes are very slightly less than this (except for lithium) — by no more than about 0.1% – 0.2%.  $^7\text{Li}$  is actually about 0.23% more massive than this estimate. How much additional error would a missing electron for a positive ion introduce? Is this significant?

Note: you can use *Mathematica* to retrieve the atomic masses of various isotopes with a function call like: `IsotopeData["Lithium7", "AtomicMass"]`.

Rearranging equation (9.4) gives

$$\frac{B^2}{V} = \left( \frac{2}{R_{eff}^2} \right) \frac{1}{e/m_{AMU}} W \quad (9.10)$$

which is a linear relationship between the an isotope's atomic weight  $W$  and your  $(B, V)$  data. Determine the set of  $B^2/V$  values for each of the isotopes from your data. Create a text data file with a single  $W$  and  $B^2/V$  pair on each line (similar to the *CurveFit* sample file *Zeeman.dat*). Use *CurveFit* to calculate the uncertainties in your multiple  $B^2/V$  data measurements for the various isotopes and fit your data to evaluate equation (9.10). Are there significant outliers in your data set? Can you figure out what went wrong for these points, if any? Are the errors correctable for at least some of these points?

Is the theory, as represented by (9.10), valid? Using the value (9.6) for  $R_{eff}$  and your fit results, determine a value for  $e/m_{AMU}$ . If the uncertainty in the value of  $R_{eff}$  is 0.2%, and the uncertainty in the Hall probe calibration magnet is also 0.2%, then what is the uncertainty in your  $e/m_{AMU}$  value (don't forget the uncertainty in the fit slope value, too)?

## PRELAB PROBLEMS

1. For  $R_{eff} = 7.35$  cm and  $V = 550$  V, what would be the magnetic field  $B$  required to detect each of the various stable isotopes of the alkali metals Na through Cs? The halogens Cl and Br? Assume the atoms are singly ionized. Which alkali metal should be most easily detected and why? Which should be the most difficult? Which element should you attempt to detect first?

The Physics 6 website folder:

[http://sophphx.caltech.edu/Physics\\_6/Extras/Mass\\_Spectrometer\\_Exp\\_9/element\\_data/](http://sophphx.caltech.edu/Physics_6/Extras/Mass_Spectrometer_Exp_9/element_data/)

contains a PDF document [atomic mass abund.pdf](#) listing atomic isotope abundances as well as a Mathematica notebook [ionization energies.nb](#) which shows how to access an element database with the information you need. It is in the folder

2. How are  $V$  and  $m$  related for ions of different masses if  $B$  is kept fixed? Assume you have detected  $^{85}\text{Rb}$  ions with  $V = 550$  V. If you *do not change the magnetic field  $B$* , then at what acceleration voltage would you expect to detect ions of  $^{87}\text{Rb}$ ? [hint: you don't need your answers to problem 1 to answer this question — the answer is easy to calculate]
3. Note that the symmetry between the acceleration voltage  $V$  and the ion mass  $m$  in equation (9.4) implies that a relation analogous to (9.7) exists between  $\Delta R$  and  $\Delta V$  (for fixed  $B$ ). For slits widths  $w = 2.5 \times 10^{-3}$  inch, what should be the minimum line width (in volts) of an ion peak centered at an acceleration potential of 550 V? [hint: relation (9.8)]
4. The magnetic field of the Hall probe calibration magnet is specified in units of *Gauss*. The SI unit you should have used for the magnetic fields you calculated in problem 1 is *Tesla*. What is the conversion factor between these two units?
5. If the desired probability that an ion will arrive at the detector without being scattered by an air molecule in its path is 95%, and the ion path length is 0.25 meter, then what is the maximum allowable number density of air molecules in the vacuum system? Assume that if an ion's center approaches within  $3\text{\AA}$  of an air molecule's center, then it will be scattered. What is the maximum allowable vacuum pressure (at 298 Kelvin)? Express your answer in Torr.
6. If the uncertainty in the slope of your fit to (9.10) is 0.5%, and the uncertainties in the Hall probe calibration and the value of  $R_{eff}$  are both 0.2%, what is the uncertainty in your  $e/m_{AMU}$  value (in %)?



## APPENDIX A: THE BEAM FOCUSING MAGNET

*Magnetic focusing*

The magnetic field not only selects among the various isotopes, it also provides focusing of the ion beam for the selected isotope between the ion gun exit slit and the beam detector entrance slit as we shall now describe. For this discussion we shall use the simplified model of a field that is uniform within a radius  $R_{eff}$  of the pole axis and 0 elsewhere, as in Figure 4 on page 9 – 4. We know that in order to make the  $90^\circ$  turn the selected ions must have a cyclotron radius of  $R_{eff}$  as well. Set up an  $x$ - $y$  coordinate system for the plane of the ions' path with its origin at the pole axis, the  $x$ -axis aligned with the incoming ion beam, and the  $y$ -axis aligned with the outgoing beam.

Selected ions approaching the magnet exactly along the  $x$ -axis follow a circular arc in the field with a center of curvature at  $(x, y) = (R_{eff}, R_{eff})$ . Now consider ions which are not approaching from exactly along the  $x$ -axis. One such ion may enter the field and follow a circular arc with its center very slightly displaced, i.e.: its center of curvature is at  $(x, y) = (R_{eff} + u, R_{eff} + v)$ , where  $u$  and  $v$  are both  $\ll R_{eff}$ . The situation (for positive  $u$  and  $v$ ) is depicted in Figure 8. We ask the following questions: could such an ion have originated from a point on the  $x$ -axis, and if so, how far is this point from the magnet, and similarly could its destination upon leaving the field be somewhere on the  $y$ -axis?

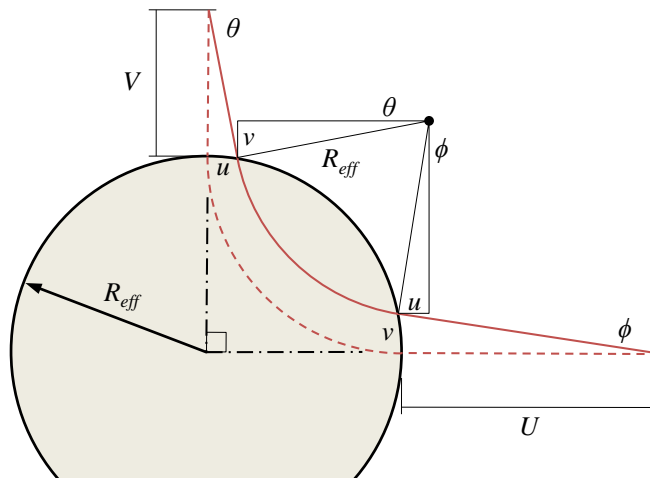


Figure 8: The geometry used to evaluate the focusing performance of the magnet.

A review of Figure 8 while keeping in mind that  $u$  and  $v$  are small should convince you that angles  $\theta$  and  $\phi$  are also small, so we can approximate  $\theta \approx v/R_{eff}$  and  $\phi \approx u/R_{eff}$ . Thus we have the similar triangles shown, and clearly the offset ion beam intersects the  $x$  and  $y$  axes with angles  $\phi$  and  $\theta$ , respectively. The distances from the edge of the magnetic field to the intersection points we call  $U$  and  $V$ , as also shown in the figure.

Thus,  $u/V = v/R_{eff}$  and  $v/U = u/R_{eff}$ . Eliminating  $u$  and  $v$  from these equations, we find that

$$UV = R_{eff}^2 \quad (9.A.1)$$

Equation (9.A.1) is independent of  $u$  and  $v$ , so if the ions are emitted by the ion gun at a distance  $U$  from the magnet through a small range of angles, they will be focused at a point a distance  $V$  from the magnet, as shown in the figure! Note that the formula (9.A.1) may be cast into a form equivalent to that for a thin optical lens of focal length  $R_{eff}$  by using the distances from the origin to the two focal points,  $U' = U + R_{eff}$  and  $V' = V + R_{eff}$ . With these definitions, (9.A.1) becomes:

$$\frac{1}{U'} + \frac{1}{V'} = \frac{1}{R_{eff}} \quad (9.A.2)$$

This ability to focus an ion beam also applies to the more realistic magnetic field model of Figure 6 on page 9–7, as is shown by the ion paths in Figure 7 on page 9–8. More about this in the next section.

### ***Magnetic field modeling***

The static magnetic field in the gap between and surrounding the pole pieces is described by the magnetostatic, current-free pair of Maxwell equations,

$$\nabla \cdot \vec{B} = 0 \quad \nabla \times \vec{B} = 0 \quad (9.A.3)$$

Thus, the field in this region may be described by a scalar potential  $\Phi_M$  which satisfies Laplace's equation:

$$\vec{B} = -\nabla\Phi_M \quad \nabla^2\Phi_M = 0 \quad (9.A.4)$$

To get the boundary condition at the surfaces of the pole pieces, where there are also no macroscopic currents, we consider the field continuity requirements set by Maxwell's equations, namely: the normal component of  $\vec{B}$  and the tangential component of  $\vec{H} = \vec{B}/\mu$  are each continuous across the boundary between the pole-piece metal and the surrounding air. To be an effective electromagnet, the pole-piece metal should have a large relative permeability  $\mu$ ; typically it is 1000s of times larger than that of the surrounding air.

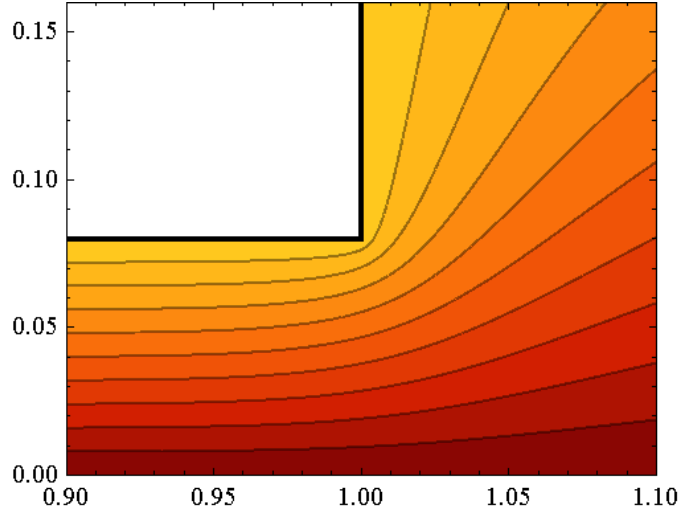


Figure 9: Model results for the magnetic scalar potential  $\Phi_M$  contour plot near the edge of a pole-piece. The plane through the center of the gap between the two pole-pieces is at the bottom edge of the figure. As explained in the text, the pole-piece surface is modeled as an equipotential  $\Phi_M = 1$ .

Inside the magnet approaching a pole-piece the magnetic field is more or less aligned with the magnet's axis, but typically has a radial component near the surface of the pole metal, especially near the cylindrical side surface. Therefore just inside the metal surfaces of the pole-pieces, which are at the ends of the magnet's core metal and are relatively far from the copper coils carrying the current generating the field, the normal component of  $\vec{B}$  is at least as large as a few  $1/10^{\text{th}}$ s of the tangential component; of course, near the pole-piece faces the field is mainly normal to the surface. The boundary conditions on the field require that the tangential component just outside the metal surface is only  $\mu_0/\mu$  that just inside the surface, so it is 1000s of times smaller, whereas the normal component is unchanged across the surface. Consequently,  $\vec{B}$  just outside the pole pieces is very nearly normal to the metal surfaces — in other words, *the pole-pieces are, to an excellent approximation, equipotential surfaces of the magnetic scalar potential  $\Phi_M$* . This is the boundary condition we seek; we set  $\Phi_M = \pm 1$  at the two pole surfaces, and the plane through the center of the gap normal to the pole axis has  $\Phi_M \equiv 0$ .

The other important boundary condition is that far from the pole piece gap (but near the  $\Phi_M \equiv 0$  plane) the field approaches that of a magnetic dipole located at the origin and aligned with the pole axis.

The pole-pieces are cylindrical, so a cylindrical coordinate system is appropriate. The azimuthal symmetry of the pole-pieces means that  $\vec{B}$  has no azimuthal component and no azimuthal variation. Thus  $\Phi_M$  is a function of  $r$  and  $z$  only, and the Laplace's equation (9.A.4) becomes

$$0 = \nabla^2 \Phi_M = \frac{1}{r} \frac{\partial}{\partial r} \left( r \frac{\partial \Phi_M}{\partial r} \right) + \frac{\partial^2 \Phi_M}{\partial z^2} = \frac{1}{r} \frac{\partial}{\partial r} \Phi_M + \frac{\partial^2 \Phi_M}{\partial r^2} + \frac{\partial^2 \Phi_M}{\partial z^2} \quad (9.A.5)$$

To solve the partial differential equation (9.A.5) we can use the *finite-difference* or *relaxation* method, which is easy to implement but fairly slow to converge to an accurate solution. This technique is implemented in *Mathematica*® code in the notebook `fastrelax.nb` available in a zip file on the Physics 6 website: [Field Models.zip](#). This file also includes field model data resulting from performing 243,000 iterations of that code saved in a large text file named `Bmatrix.dat`; this file is used by the other notebooks in the zip file. Figure 9 is a contour plot of the modeled  $\Phi_M$  near one of the pole-piece edges.

The magnetic field model may be visualized in various ways; the notebook `relax field plots.nb` gives some examples. Figure 10 is a depiction of the magnetic field near the edge of the gap between the pole-pieces.

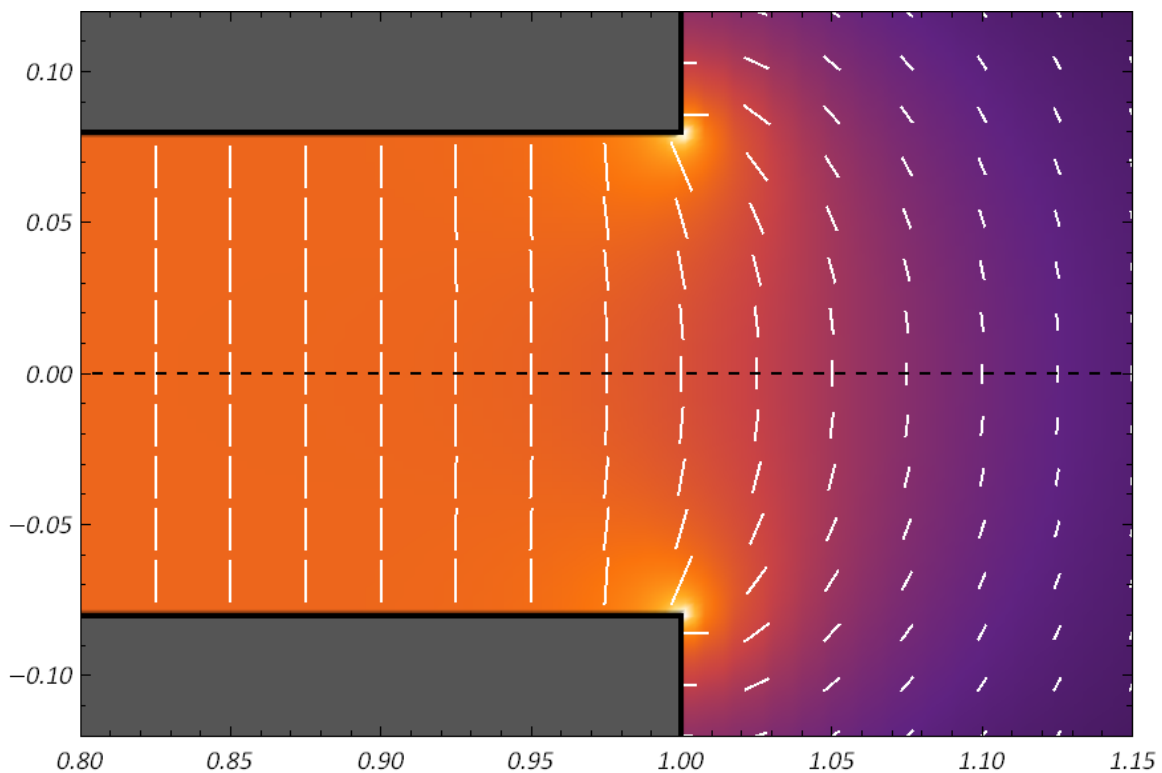


Figure 10: The magnetic field near the edge of the gap between the pole pieces. The white lines represent field vectors at the points near their centers; the strength of the field is indicated by the lengths of the lines and the background colors. The units of length are in terms of the pole-piece radius.

By numerically calculating ion trajectories through the magnetic field model you can determine the effective radius  $R_{eff}$  and evaluate the ion beam focusing characteristics of the magnet. The notebook `relax trajectory.nb` was written to perform these calculations.